Permeability of One-Dimensional Potential Barriers

By R. J. Le Roy*

Theoretical Chemistry Institute and Chemistry Dept., University of Wisconsin, Madison, Wisconsin 53706

AND

K. A. Quickert † and D. J. Le Roy

Lash Miller Chemical Laboratories, University of Toronto, Toronto 181, Ontario, Canada

Received 13*th April* 1970

A numerical method is described for computing the exact permeability (tunnelling probability) for any one-dimensional potential barrier. It is used to test the validity of the widely-used approximate formulae for the tunnelling factors for truncated parabolic barriers. The method is also used to calculate tunnelling factors for the $H+H_2$ exchange reaction, using the theoretical potential surface of Shavitt, Stevens, Minn and Karplus, and it is shown that standard Eckart and parabolic barrier approximations can yield considerable error.

Evaluation of the probability of transmission for a particle impinging on a potential barrier has long been an important problem in the theoretical treatment of chemical reaction rates. The early use of tunnelling corrections is discussed by Glasstone, Laidler and Eyring.[1] Their usefulness in interpreting the results of proton transfer reactions has been reviewed by Caldin,[2] and their application to the hydrogen exchange reactions is discussed by Johnston.[3]

While the potential barrier in a chemical reaction is in general multi-dimensional, a widely-used approximation has been to consider the reaction as motion along a one-dimensional (1-Dim) "reaction coordinate" which is orthogonal to all other modes of motion of the interacting species. In this approximation, estimates of barrier transmission rates have usually been obtained after approximating the exact potential by a model 1-Dim barrier of one of two analytic forms for which exact analytic tunnelling probabilities are known : an Eckart barrier,[4] or an infinite parabolic barrier.[5] An exact tunnelling probability expresson has also been derived [6] for a third potential form, the infinite double anharmonic barrier, $V(x) = V_0[1-(x/a-a/x)^2]$; however, this result has not yet been applied to chemical problems. Although the result for the parabolic potential is for an infinite barrier, it has been widely used for truncated parabolas,[2] probably because of the convenient analytic expression obtained for the tunnelling factor in the high-temperature limit.[7] The Eckart potential,[4] on the other hand, is finite, and the potential and its first derivative are everywhere continuous; however, while its exact transmission probability is known analytically, the tunnelling factors cannot be obtained in closed form.‡

* present address: Dept. of Physics, University of Toronto, Toronto 181, Ontario, Canada.

† present address: Institut für Physikalische Chemie, Universität Göttingen, 34 Göttingen, Bürgerstrasse 50, West Germany.

‡ A table of Eckart tunnelling factors for a wide range of potential parameter values and reduced temperatures is given in ref. (3), p. 44. Johnston (private communication, 1969) computed this table using the correct transmission probability expression and not his [3] eqn (2-22), in which the last term should be $\pi^2/4$, not $2\pi^2/16$.

Despite the convenience of using the analytic [7] or tabulated [3] results for the two main model barriers mentioned above, these potentials will rarely accurately represent a reasonable 1-Dim cut through an actual potential surface. Furthermore, the analytic tunnelling probabilities can not take account of the change in the asymptotic reduced mass between reagents and products which arises in many chemical situations. An additional problem associated with the use of Bell's formulae [7] for parabolic barriers is the unknown effect of truncating the barrier at a finite height on the transmission probability, and hence on his approximate expressions for the tunnelling factor.

In the next section, a simple numerical procedure is presented for determining exact transmission coefficients for any 1-Dim potential barrier. This approach is tested by comparing its predictions to the exact analytic results for an Eckart barrier.[4] The numerical method is then applied to truncated parabolic barriers to examine the validity of Bell's approximations. Finally, the usefulness of the exact 1-Dim method is demonstrated by applying it to the calculation of tunnelling factors for the $H+H_2$ exchange reaction.

SCATTERING BY A ONE-DIMENSIONAL BARRIER

EXACT BARRIER PASSAGE PROBABILITY

Many elementary quantum mechanics texts derive the exact transmission probability for a rectangular barrier,[8] and the present treatment is qualitatively the same.* The Schrödinger equation describing 1-Dim potential scattering may be written in the dimensionless form

$$d^2\psi(y)/dy^2 + B_y[\bar{E} - \bar{V}(y)]\psi(y) = 0, \quad (1)$$

where

$$y = x/a,\ \bar{E} = E/V_0,\ \bar{V}(y) = V(x)/V_0,$$

and

$$B_y = 2\mu V_0 a^2/\hbar^2 = 20.746\ 59\mu[\text{a.m.u.}]V_0[\text{kcal/mol}]\ (a[\text{Å}])^2.$$

In general, the energy and length scaling factors V_0 and a may be chosen completely arbitrarily; however, it is usually convenient to associate them with the barrier height and width. In the present discussion, the coordinate x along the reaction path is

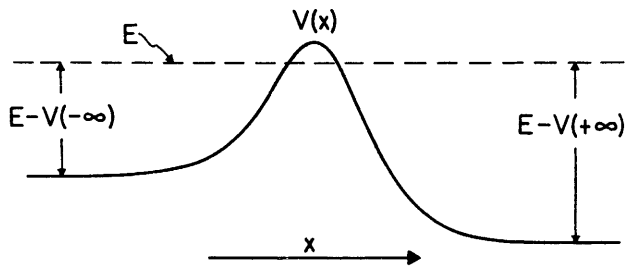

FIG. 1.—Schematic potential barrier.

defined such that $x \simeq -\infty$ corresponds to reagents and $x \simeq +\infty$ to products. The potential $V(x)$ is everywhere finite and approaches constant values in the limits $x \simeq \pm\infty$ (see fig. 1). E is the relative energy of the colliding particles. In

* A. Kuppermann has pointed out that a method similar to that described here was previously presented and used in a study of the Shottky effect.[9]

general, the effective reduced mass μ may vary along the reaction coordinate, and the asymptotic reduced mass of the reagents may differ from that of the products.[10] However, this may readily be taken account of by introducing a variable mass $\mu = \mu(y)$ into eqn (1), or alternatively by scaling the reaction coordinate appropriately while holding μ fixed.[11] When this question arose here the latter approach was used, and hence μ is assumed to be a constant in the rest of the derivation.

For " reagents ", the solution of eqn (1) may be asymptotically expressed as a linear combination of plane waves incident on and reflected from the barrier, i.e., for $y \simeq -\infty$:

$$\psi(y) = A_{\mathrm{I}} \exp(i\alpha_- y) + A_{\mathrm{R}} \exp(-i\alpha_- y), \tag{2}$$

where $\alpha_- = \{B_y[\bar{E} - \bar{V}(-\infty)]\}^{\frac{1}{2}}$. Similarly, particles which tunnel past the barrier to form products may be described asymptotically by a plane wave moving away from the barrier, i.e., for $y \simeq +\infty$:

$$\psi(y) = A_{\mathrm{T}} \exp(i\alpha_+ y), \tag{3}$$

where $\alpha_+ = \{B_y[\bar{E} - \bar{V}(+\infty)]\}^{\frac{1}{2}}$. The probability of barrier passage is the ratio of the transmitted to the incident flux :

$$\kappa(\bar{E}) = \frac{v_+}{v_-} \left| \frac{A_T}{A_{\mathrm{I}}} \right|^2,$$

where v_+ and v_- are respectively the asymptotic velocities of products (+) and reagents (−). For fixed μ, $v_+/v_- = \alpha_+/\alpha_-$, and hence

$$\kappa(\bar{E}) = \frac{\alpha_+}{\alpha_-} \left| \frac{A_T}{A_{\mathrm{I}}} \right|^2. \tag{4}$$

To facilitate computation of $\kappa(\bar{E})$ it is convenient to expand $\psi(y)$ in terms of its real and imaginary parts :

$$\psi(y) = \phi_1(y) + i\phi_2(y),$$

Comparing this with eqn (3) shows that for products, at $y \simeq +\infty$:

$$\begin{aligned} \phi_1(y) &= A_{\mathrm{T}} \cos(\alpha_+ y), \\ \phi_2(y) &= A_{\mathrm{T}} \sin(\alpha_+ y). \end{aligned} \tag{5}$$

Starting from this boundary condition with an arbitrary choice of A_{T} (most conveniently, $A_{\mathrm{T}} \equiv 1$), the two independent solutions $\phi_1(y)$ and $\phi_2(y)$ may be numerically integrated through the barrier to the reagent boundary condition at $y \simeq -\infty$. There they may be decomposed into

$$\begin{aligned} \phi_1(y) &= C_1 \cos(\alpha_- y) + D_1 \sin(\alpha_- y), \\ \phi_2(y) &= C_2 \cos(\alpha_- y) + D_2 \sin(\alpha_- y). \end{aligned} \tag{6}$$

Comparing eqn (2) and (6), values of A_{I} and A_{R} are obtained in terms of values of the solution functions $\phi_1(y)$ and $\phi_2(y)$ at adjacent integration mesh points y_1 and y_2. Substituting them into eqn (4) yields

$$\begin{aligned} \kappa(\bar{E}) = 4(\alpha_+/\alpha_-) \sin^2[\alpha_-(y_2 - y_1)] \,|\, A_{\mathrm{T}} \,|^2 \{ &[\phi_1(y_1)]^2 + [\phi_1(y_2)]^2 + [\phi_2(y_1)]^2 + \\ &[\phi_2(y_2)]^2 - 2[\phi_1(y_1)\phi_1(y_2) + \phi_2(y_1)\phi_2(y_2)] \cos[\alpha_-(y_2 - y_1)] + \\ &2[\phi_1(y_1)\phi_2(y_2) - \phi_1(y_2)\phi_2(y_1)] \sin[\alpha_-(y_2 - y_1)] \}^{-1}. \end{aligned} \tag{7}$$

This is the desired result. The exact numerical integration of eqn (1) and the practical application of the boundary conditions are discussed below.

The above method was tested by applying it to a symmetric Eckart barrier, $\bar{V}(y) = 1/\cosh^2(y)$, for which the exact $\kappa(\bar{E})$ function is known analytically.[4] For barriers with B_y values ranging from 2 to 200, it was found that single precision numerical integration yielded $\kappa(\bar{E})$ accurate to within 1×10^{-5}, for $\bar{E} = 0.1$, 1.0, and 2.0. This confirms the validity of the present approach.

INTEGRATION OF EQN (1) AND APPLICATION OF BOUNDARY CONDITIONS

The Numerov method [12] is a very efficient technique for the numerical integration of a homogeneous linear second-order differential equation without first derivatives, such as eqn (1).[13] One restriction on its use is that it assumes that the potential function $\bar{V}(y)$ is smooth, since, when it is not, an inordinately small increment of integration is required to yield reasonable accuracy. In the latter situation a self-starting technique such as the Runge-Kutta-Gill (RKG) method [14] is more appropriate. The RKG procedure requires more arithmetic, and one more function evaluation per integration step than does the Numerov method. However, when calculating the solution at a given point the latter utilizes the solution at the *two* previous mesh points, while the former requires the solution and its first derivative only at the adjacent previous point. Thus, if RKG is used and the integration mesh chosen so that no mesh points lie at any potential slope discontinuities, the numerical integration is in no way affected by the existence of such discontinuities. In the present work, the RKG procedure was used in the calculations for truncated parabolic barriers, as they have discontinuous first derivatives at $y = \pm 1$ (see below). The Numerov method was used in all other cases.

For either algorithm the accuracy of the integration improves with decreasing increment Δy until a lower bound is reached beyond which the theoretical improvement in the numerical accuracy is exceeded by the accumulated machine round-off error. The optimum increment of integration as a function of particle and barrier size is approximately given by

$$\Delta y = \Delta x/a = F/(B_y)^{\frac{1}{2}},$$

where the height of the barrier is used as V_0 in the calculation of B_y. The value of the numerical constant F depends on the integration algorithm and the number of significant digits of machine accuracy. On the 8-digit computer used in the present work, $F = 0.18$ was appropriate for Numerov integration, and $F = 0.07$ for the RKG algorithm.

For potentials with a finite range, such as truncated parabolic barriers, application of the boundary conditions eqn (2) and (3) presents no difficulties. On the other hand, realistic potentials which reach their asymptotic values only in the limits $y \simeq \pm\infty$ can only be integrated over a finite interval, and hence the exact boundary conditions are never achieved. In the present work, the ends of this finite interval, y_- and y_+, were defined as the smallest values of $|y|$ for which the first-order WKB convergence criterion (see, e.g., pp. 112-115 of ref. (8*a*)) was smaller than a chosen critical value. Thus, they are the solutions of

$$\left| [\alpha(y)]^{-2} \frac{d}{dy}\alpha(y) \right| = Z,$$

where $\alpha(y) = \{B_y[\bar{E} - \bar{V}(y)]\}^{\frac{1}{2}}$ and Z is the chosen convergence criterion. It was found here that $Z = 1.0 \times 10^{-5}$ yielded values of $\kappa(\bar{E})$ within 1×10^{-5} of the exact analytic barrier passage probabilities for Eckart barriers of different sizes. A Fortran listing of the subroutine used to integrate eqn (1) to yield $\kappa(\bar{E})$ is given in the appendix to ref. (15).

THE TUNNELLING FACTOR $\Gamma(T)$

The tunnelling factor is the ratio of the quantum mechanical to the classical barrier-crossing rate for particles with a Boltzmann distribution of initial kinetic energies relative to the barrier. In reduced units analogous to those of eqn (1), it may be written as [3]

$$\Gamma(\bar{T}) = \frac{1}{\bar{T}}\int_0^\infty \kappa(\bar{E}) \exp\left(\frac{1-\bar{E}}{\bar{T}}\right) d\bar{E} \tag{8}$$

where $\bar{T} = kT/V_0$, and V_0 is the barrier height. After obtaining $\kappa(\bar{E})$ values over a range of energies by the method presented above, eqn (8) may be integrated numerically. This quantity is in effect an observable and is the point of comparison between theoretical and experimental estimates of tunnelling.

APPLICATION TO PARABOLIC BARRIERS

The potential form which appears to have been most widely used to account for tunnelling in chemical processes [2] is the truncated parabola:

$$\begin{aligned} \bar{V}(y) &= 1-y^2 \qquad \text{for } -1 \leqslant y \leqslant 1 \\ &= 0 \qquad\quad \text{for } |\,y\,| < 1, \end{aligned} \tag{9}$$

where particles may impinge on the barrier with energies $\bar{E} > 0$. In the present discussion, the energy and length scaling factors V_0 and a used in B_y always signify the barrier height, and the half-width at its base. It is apparent that in this case the transmission probability function $\kappa(\bar{E})$ is completely defined by the appropriate value of B_y, since eqn (1) is precisely the same for all barriers with different heights and widths, but the same B_y.

It will be convenient to replace B_y by the previously used [2, 7] and equivalent reduced parameter

$$\beta = \pi(B_y)^{\frac{1}{2}} = 14.309\,46\,(\mu[\text{a.m.u.}]V_0[\text{kcal/mol}])^{\frac{1}{2}}a[\text{Å}] = 2197.524V_0[\text{kcal/mol}]/\nu[\text{cm}^{-1}]$$

where ν is the characteristic frequency of the harmonic oscillator potential obtained on inverting the parabolic barrier.* The reduced temperature $\bar{T}$ used here is equivalent to the previously used [2, 7] reduced variable $\alpha = 1/\bar{T}$. In the following discussion, particular combinations of temperature, and particle mass and barrier size are characterized by values of $\bar{T}$ and β. For given choices of these quantities, exact values of $\kappa(\beta,\bar{E})$ and $\Gamma(\beta,\bar{T})$ were calculated by the numerical method presented above.

The exact transmission probability [5] for particles impinging on an *infinite* parabolic barrier: $\bar{V}(y) = 1-y^2$, where $-\infty < y < +\infty$, is

$$\kappa_\infty(\beta,\bar{E}) = \{1+\exp[\beta(1-\bar{E})]\}^{-1}, \tag{10}$$

where $\bar{E}$ and β are as defined above, and $\bar{E}$ may range to $\pm\infty$. A widely used approximation has been to assume that the transmission coefficient for a *finite* parabolic barrier may be accurately represented by eqn (10). This question is examined in fig. 2 where the ratios of approximate (from eqn (10)) to exact numerical (κ_{ex}) transmission coefficients are plotted against $\bar{E}$ for barriers of different sizes (different β). The error inherent in the use of $\kappa_\infty(\beta,\bar{E})$ for finite barriers increases with decreasing β, and for the particle and barrier sizes considered, eqn (10) becomes satisfactory

* While consideration of eqn (1) suggests that B_y is a more " natural " parameter, previous work with truncated parabolas [2, 7] used β, which is a natural parameter in Bell's [7] approximate analytic tunnelling factor expressions.

only for energies above the top of the barrier ($\bar{E}>1$). However, in all cases it is significantly in error at low values of $\bar{E}$, and this will affect the tunnelling factors at low temperatures.

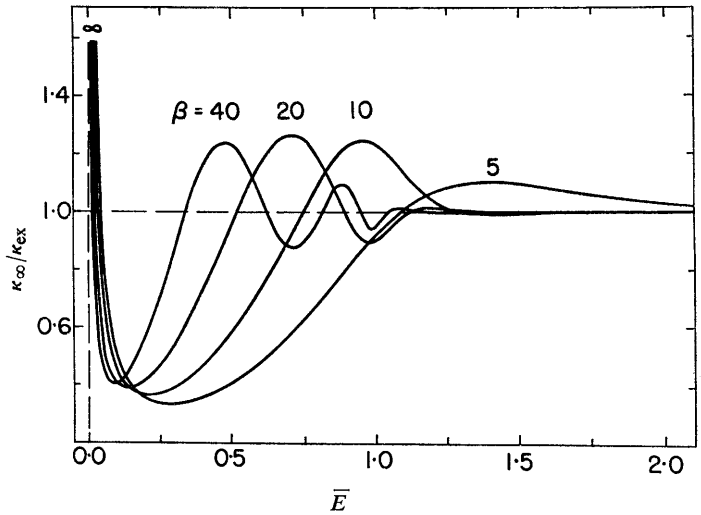

FIG. 2.—Ratios of approximate (κ_∞) to exact numerical (κ_{ex}) transmission probabilities for truncated parabolic barriers, as a function of the reduced energy $\bar{E}$. The barrier maxima correspond to $\bar{E}=1$.

Bell's [7] widely used formulae for the tunnelling factors for truncated parabolic barriers are based on eqn (10). On substituting it into eqn (8) he obtained an analytic approximation for the resulting integral, yielding

$$\Gamma^{I}_{\infty}(\beta,\bar{T}) = \frac{\pi/\beta\bar{T}}{\sin(\pi/\beta\bar{T})} - \frac{\exp(1/\bar{T}-\beta)}{\beta\bar{T}-1}\times \left\{1-\left(\frac{1-\beta\bar{T}}{1-2\beta\bar{T}}\right)e^{-\beta}+\left(\frac{1-\beta\bar{T}}{1-3\beta\bar{T}}\right)e^{-2\beta}-\ldots\right\}. \quad (11)$$

Although individual terms in this expansion have singularities at integer values of $1/\beta\bar{T}$, there is exact mutual cancellation of such terms so that the sum remains finite and eqn (11) is defined for all values of $\beta\bar{T}$.* Bell also noted [7] that in the high temperature region where

$$\left|\frac{\exp(1/\bar{T}-\beta)}{\beta\bar{T}-1}\right| \ll 1,$$

$\Gamma^{I}_{\infty}(\beta,\bar{T})$ becomes

$$\Gamma^{II}_{\infty}(\beta,\bar{T}) = \frac{\pi/\beta\bar{T}}{\sin(\pi/\beta\bar{T})}, \quad (12)$$

which has been used widely.[2, 10] The accuracies of these approximate formulae are illustrated in fig. 3, where their predictions are compared to the exact numerical values $\Gamma_{ex}(\beta,\bar{T})$; the solid curves used eqn (11) for Γ_∞, and the broken curves eqn (12). The breaks in the solid curves at integer values of $1/\beta\bar{T}$ are a reminder that two of the terms in the full expansion of the right side of eqn (11) are singular at each of these points.

* In Bell's original treatment [7] he unnecessarily [2] restricted the use of eqn (11) to $\beta\bar{T}>1$.

The effects shown in fig. 3 reflect the trends seen in fig. 2, the errors in the approximate formulae increasing with decreasing β and $\bar{T}$. For all barriers, the simple approximate formula Γ^{II}_{∞} is as good as the more general expression Γ^{I}_{∞} *wherever* the latter is reasonably accurate. For the larger barriers ($\beta \gtrsim 20$), this appears to

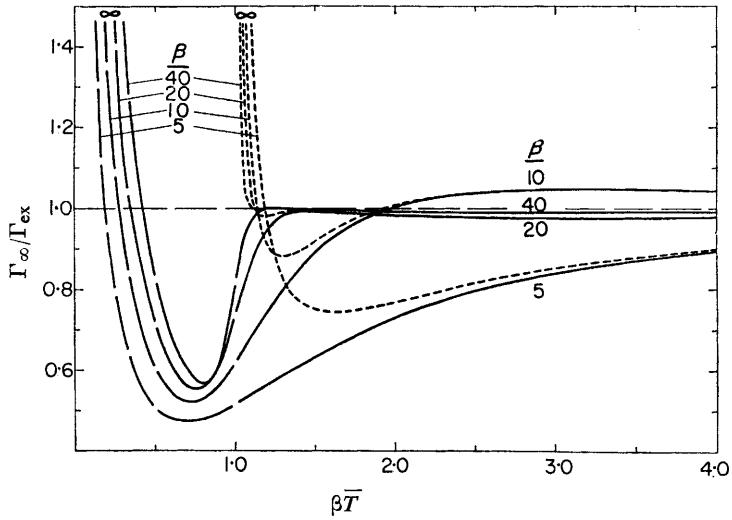

FIG. 3.—Ratios of approximate (Γ_{∞}) to exact numerical (Γ_{ex}) tunnelling factors for truncated parabolic barriers. The solid curves were obtained by using eqn (11) for Γ_{∞}, and the broken curves, eqn (12). The breaks in the former for $\beta\bar{T} \leqslant 1$ correspond to the points at which pairs of terms in eqn (11) blow up (i.e., where $1/\beta\bar{T}$ is an integer).

include virtually all $\bar{T} > 1/\beta$. On the other hand, for all barrier sizes, none of the approximate formulae are at all reliable for $\bar{T} < 1/\beta$.* In addition to Γ^{I}_{∞} and Γ^{II}_{∞}, this includes eqn (7) and (10) in Bell's paper,[7] which were suggested for use in this region. The former, proposed for $\bar{T} < 1/\beta$, yields curves of $\Gamma_{\infty}/\Gamma_{ex}$ which are identical to those for Γ^{I}_{∞} from $\beta\bar{T} = 0$ to approximately their minima, and then rise to infinity at $\beta\bar{T} = 1$. The latter, designed for $\bar{T} \approx 1/\beta$, yields negative values of $\Gamma_{\infty}/\Gamma_{ex}$ for all $\bar{T}$ outside a very narrow interval about $\bar{T} = 1/\beta$, and even in this interval it is significantly less accurate than is Γ^{I}_{∞}.

To put the present results in perspective it is helpful to consider Caldin's [2] table VII, which contains most of the reliable data on the dimensions of energy barriers for proton transfer reactions. For all of the cases presented there $\beta \gtrsim 30$, and the temperatures corresponding to $\beta\bar{T} = 1$ range between 130 and 250 K. Since most of the results were obtained using Γ^{II}_{∞} (eqn (12)),[2] the experimental data for these cases must have corresponded to $\beta\bar{T} > 1$, and fig. 3 suggests that their derived barrier parameter should be reasonably accurate. However, the present results clearly demonstrate that in those cases for which eqn (11) *had* to be used (where $\beta\bar{T} \lesssim 1$), the reported barrier parameters are probably unreliable.

Another situation in which Bell's [7] approximate formulae have been used is in calculating tunnelling corrections to the rates of the isotopic $H + H_2$ exchange reactions. Weston [16] fitted a parabola to the reaction path at the saddle point of a Sato [17] potential surface for collinear collisions, and used Bell's formulae [7] to estimate

* In addition to the results shown in fig. 3, a calculation for $\beta = 80$ showed that its $\Gamma^{I}_{\infty}/\Gamma_{ex}$ curve has a minimum of 0.57 at $\beta\bar{T} = 0.84$, while for all $\beta\bar{T} \gtrsim 1.05$ it is within 1 % of unity.

the tunnelling through it. This parabolic barrier was 8.0 kcal/mol high and had $\beta = 11.64$, so that $\overline{T} = 1/\beta$ corresponded to 340 K. Using the present method it was found that Weston's [16] predicted tunnelling factors at 1000, 500, and 295 K are respectively 6 % larger, and 6 and 35 % smaller than the exact tunnelling factors for his barrier.

APPROXIMATION OF BARRIERS BY ECKART AND PARABOLIC FUNCTIONS

RESULTS FOR $H + H_2$

This section examines the validity of approximating an actual barrier with a convenient analytic function, by considering the tunnelling contribution to the rate of the simple hydrogen exchange reaction. Here the exact 1-Dim barrier is taken as the minimum potential path on the potential surface for collinear collisions. A number of treatments have previously estimated the amount of tunnelling in this system using Eckart [3, 10, 18-20] or parabolic [10, 16] approximations to the actual potential barrier.

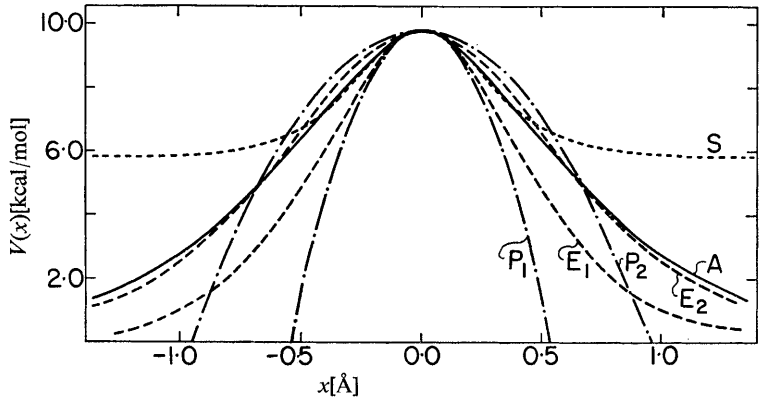

FIG. 4.—Comparison of actual theoretical 1-Dim potential barrier for collinear $H+H_2$ collisions (curve A) with analytic approximations to it. Curves P_1 and P_2 are truncated parabolas corresponding to $\beta = 14.74$ and 24.84, respectively, while curves E_1 and E_2 are Eckart functions, $V(x) = V_0/\cosh^2(x/a)$, with $a = 0.566$ and 0.768 Å respectively. E_1 and P_1 have the same curvature at the maximum as does curve A, while E_2 and P_2 have the same width at half maximum. Curve S is the Eckart function with which Shavitt [19] approximated the barrier for this case.

The potential surface used here is the one reported by Shavitt, Stevens, Minn and Karplus,[21] scaled by a factor of 0.89 as recommended by Shavitt.[19] The method of obtaining the present 1-Dim barrier from the low-energy path on this surface is described elsewhere.[11] Fig. 4 shows the actual energy barrier so obtained, curve A, and five approximations to it. Curves E_1 and P_1 are respectively Eckart and parabolic potentials with both the same height and curvature (second derivative) at the maximum as the "exact" barrier. Similarly, curves E_2 and P_2 are Eckart and parabolic barriers chosen to have the same height, and the same width at half maximum as the actual curve. The additional curve, S, is the Eckart function Shavitt [19] used in estimating tunnelling factors for this case. His potential had the same curvature at the maximum as the actual barrier, and was "selected by inspection to give a good fit to the *ab initio* barrier over as much of its upper part as possible". The constant reduced mass used with these potentials is $\mu = M_H/3 = 0.335\,94$ a.m.u.

Fig. 5 shows the calculated tunnelling factors for these potentials as a function of temperature; the curves are labelled as in fig. 4. The total computer time required

to generate curve A was less than 1 min on an IBM–7094. As might be expected, the present Eckart tunnelling factors (curves E_1 and E_2) are closer to the exact values than are the parabolic results. However, none of the present approximate barriers yields tunnelling factors that are good, especially at low temperatures. On the other hand, the manner in which the approximate results straddle curve A (in fig. 5) suggests that their main source of error lies in the criteria used to fit the approximate barriers to the actual one. This is confirmed by the fact that Shavitt's Eckart function [19] yielded tunnelling factors in remarkable agreement with the present exact values, despite the large differences between his barrier and the actual one. Furthermore, it seems certain that systematic variation of the two free Eckart parameters could yield even better agreement with curve A. By comparison, it was found that no truncated parabola would yield tunnelling factors in good agreement with curve A over the whole temperature range shown. The best fit of this sort (corresponding to $\beta \simeq 19$) had $\Gamma(T)$ values which were significantly too small at high temperatures and too large at low. Thus, while the tunnelling factors for the $H+H_2$ case are insensitive to the nature of an approximating barrier except near its maximum, they are *very* sensitive to its shape in this region. In any case, exact numerical computations of $\Gamma(T)$ should be used whenever the shape of the barrier is known.

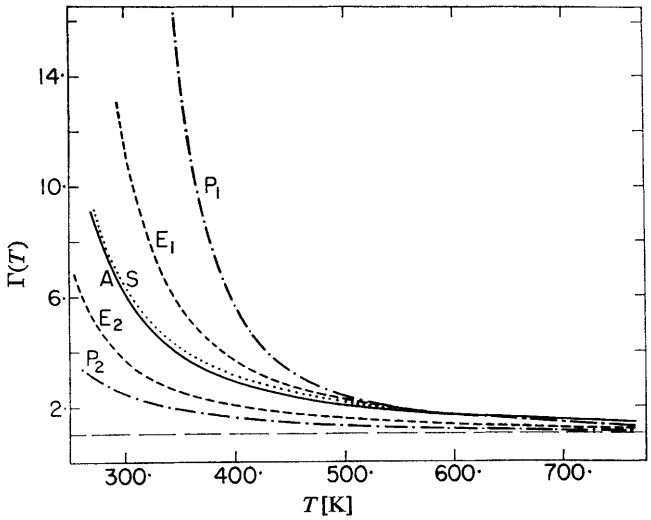

FIG. 5.—Tunnelling factors for the potentials shown in fig. 4, labelled in the same manner. The broken horizontal line lies at unity.

CONCLUDING REMARKS

A method has been presented for calculating the exact transmission probabilities and tunnelling factors for any 1-Dim potential barrier. It has been used to determine the region of validity of Bell's [7] approximate expressions for the tunnelling factors for truncated parabolic barriers. It has also been used elsewhere [11] to help correlate with theory some new experimental measurements of the relative rates of the exchange reactions $H+H_2$ and $H+D_2$.

The systems in which Bell's [7] formulae are appropriate are precisely those in which there is relatively little barrier transmission except at energies close to and above its maximum. This insensitivity of such results to the nature of the potential except near its maximum is further illustrated by the success of Shavitt's [19] approximation for the $H+H_2$ tunnelling, discussed in the preceding section. This suggests

that if experimental results may be accurately explained using eqn (11) or (12) for values of β and $\overline{T}$ for which these expressions accurately reflect the appropriate truncated parabola (e.g., $\beta \gtrsim 20$ and $\overline{T} > 1/\beta$), then the truncated parabola so obtained accurately approximates the shape and height of the actual 1-Dim potential barrier near its maximum.

The above quantitative confirmation of the validity of eqn (11) and (12) for large barrier situations (negligible tunnelling at low energies) will be reassuring to experimentalists who have been interpreting their data using these expressions. Also, the present method offers a way of treating cases where tunnelling is important at energies well below the barrier maximum, but for which the Eckart functions results are not sufficient. However, the whole of the present approach is based on the strong assumption that a multi-dimensional problem may be meaningfully represented in 1-Dim. The validity of this approximation has been examined by Truhlar and Kuppermann.[22]

This work was supported in part by National Aeronautics and Space Administration Grant NGL 50–002–001. The authors are also grateful to the National Research Council of Canada for support, and for the award of scholarships to two of us (R. J. L. and K. A. Q.). In addition, we thank Dr. R. L. Le Roy for helpful comments on the manuscript, and R. J. L. gratefully acknowledges the encouragement of Prof. R. B. Bernstein.

[1] S. Glasstone, K. J. Laidler and H. Eyring, *The Theory of Rate Processes* (McGraw-Hill, New York, 1941).
[2] E. F. Caldin, *Chem. Rev.*, 1969, **69**, 135.
[3] H. S. Johnston, *Gas Phase Reaction Rate Theory* (Ronald Press, New York, 1966).
[4] C. Eckart, *Phys. Rev.*, 1930, **35**, 1303.
[5] (*a*) E. C. Kemble, *The Fundamental Principles of Quantum Mechanics with Elementary Applications* (McGraw-Hill, New York, 1937), §21j; (*b*) L. D. Landau and E. M. Lifschitz, *Quantum Mechanics-Non Relativistic Theory*, 2nd ed. (Pergamon Press, London, 1965), p. 176.
[6] K. A. Quickert and D. J. Le Roy, *J. Chem. Phys.*, 1970, **52**, 856.
[7] R. P. Bell, (*a*) *Trans. Faraday Soc.*, 1959, **55**, 1; (*b*) the discussion in chap 11 of *The Proton in Chemistry* (Cornell University Press, Ithaca, New York, 1959).
[8] (*a*) E. Merzbacher, *Quantum Mechanics* (John Wiley & Sons, New York, 1961), pp. 91-93; (*b*) W. Kauzmann, *Quantum Chemistry* (Academic Press Inc., New York, 1957), pp. 195-198; (*c*) A. S. Davydov, *Quantum Mechanics*, (Pergamon Press, Toronto, 1965), § 26; (*d*) see also pp. 38-47 in ref. (3).
[9] G. G. Belford, A. Kuppermann, and T. E. Phipps, *Phys. Rev.*, 1962, **128**, 524.
[10] D. J. Le Roy, B. A. Ridley and K. A. Quickert, *Disc. Faraday Soc.*, 1967, **44**, 92.
[11] (*a*) K. A. Quickert, *Ph.D. Thesis* (University of Toronto, 1970); (*b*) K. A. Quickert and D. J. Le Roy, *J. Chem. Phys.*, 1970, **53**, 1325.
[12] see e.g., R. W. Hamming, *Numerical Methods for Scientists and Engineers* (McGraw-Hill, New York, 1962), p. 215.
[13] (*a*) J. W. Cooley, *Math. Computations*, 1961, **15**, 363; (*b*) J. K. Cashion, *J. Chem. Phys.*, 1963, **39**, 1872.
[14] S. Gill, *Proc. Cambr. Phil. Soc.*, 1951, **47**, 96.
[15] R. J. Le Roy, K. A. Quickert, and D. J. Le Roy, *University of Wisconsin Theoretical Chemistry Institute Report* WIS-TCI-384 (1970).
[16] R. E. Weston, Jr., *J. Chem. Phys.*, 1959, **31**, 892.
[17] S. Sato, *J. Chem. Phys.*, 1955, **23**, 592 and 2465.
[18] I. Shavitt, *J. Chem. Phys.*, 1959, **31**, 1359.
[19] I. Shavitt, *J. Chem. Phys.*, 1968, **49**, 4048.
[20] E. M. Mortensen, *J. Chem. Phys.*, 1968, **48**, 4029.
[21] I. Shavitt, R. M. Stevens, F. L. Minn and M. Karplus, *J. Chem. Phys.*, 1968, **48**, 2700.
[22] (*a*) D. G. Truhlar, *Ph.D. Thesis* (California Institute of Technology, 1970); (*b*) D. G. Truhlar and A. Kuppermann, *J. Chem. Phys.*, 1970, **52**, 3841,